HHS Public Access

Author manuscript

Int J Cancer. Author manuscript; available in PMC 2017 February 15.

Published in final edited form as:

Int J Cancer. 2016 February 15; 138(4): 901–911. doi:10.1002/ijc.29823.

Human papillomavirus capsids preferentially bind and infect tumor cells

Rhonda C. Kines[1,*], **Rebecca J. Cerio**[2,*], **Jeffrey N. Roberts**[2], **Cynthia D. Thompson**[2], **Elisabet de Los Pinos**[1], **Douglas R. Lowy**[2], and **John T. Schiller**[2]

[1]Aura Biosciences, Cambridge, MA 02140, USA

[2]Laboratory of Cellular Oncology, Center for Cancer Research, National Cancer Institute, National Institutes of Health, Bethesda, MD 20892, USA

Abstract

We previously determined that human papillomavirus (HPV) virus-like particles (VLPs) and pseudovirions (PsV) did not, respectively, bind to or infect intact epithelium of the cervicovaginal tract. However, they strongly bound heparin sulfate proteoglycans (HSPG) on the basement membrane of disrupted epithelium and infected the keratinocytes that subsequently entered the disrupted site. We here report that HPV capsids (VLP and PsV) have the same restricted tropism for a wide variety of disrupted epithelial and mesothelial tissues, whereas intact tissues remain resistant to binding. However, the HPV capsids directly bind and infect most tumor-derived cell lines *in vitro* and have analogous tumor-specific properties *in vivo*, after local or intravenous injection, using orthotopic models for human ovarian and lung cancer, respectively. The pseudovirions also specifically infected implanted primary human ovarian tumors. Heparin and ι-carrageenan blocked binding and infection of all tumor lines tested, implying that tumor cell binding is HSPG-dependent. A survey using a panel of modified heparins indicate that N-sulfation and, to a lesser degree O-6 sulfation of the surface HSPG on the tumors are important for HPV binding. Therefore, it appears that tumor cells consistently evolve HSPG modification patterns that mimic the pattern normally found on the basement membrane but not on the apical surfaces of normal epithelial or mesothelial cells. Consequently, appropriately modified HPV VLPs and/or PsV could be useful reagents to detect and potentially treat a remarkably broad spectrum of cancers.

Keywords

Human papillomavirus; heparan sulfate proteoglycans; tumor tropism

INTRODUCTION

There were an estimated 14.1 million new cancer diagnoses and 8.2 million cancer-related deaths reported in 2012, making cancer one of the leading causes of death worldwide [1]. In

Corresponding Author: John T. Schiller, Laboratory of Cellular Oncology, NCI, NIH, 9000 Rockville Pike, Building 37, Room 4106, Bethesda, MD 20892, Phone: +1-301-496-6539, Fax: +1-301-480-5322, schillej@dc37a.nci.nih.gov.

*RCK and RJC contributed equally to this work.

recent years, there has been a tremendous effort towards understanding cancer biology and this has led to the rapid advancement of a variety of cancer treatments. However, management options for many solid tumors, such as ovarian and lung cancer, remain limited and rely heavily on traditional surgery, radiotherapy, and chemotherapy. These treatments are often hampered by drug resistance, relapse and failure to detect malignancies in the earliest, most treatable stages [2, 3]. Additional tools for cancer detection and therapy are urgently needed for primary and metastatic tumors. Here we present data showing that the use of HPV virus-like particles (VLP) and pseudovirions (PsV) might advance these goals.

HPV VLP are 55 nm capsids composed of the HPV L1 or L1 and L2 structural proteins. Additionally, preparations can be made in which L1/L2 particles encapsidate reporter gene plasmids of a limited size (<8 Kb) during self-assembly, resulting in an HPV PsV. Although PsV are non-replicative, as they do not contain any viral genes [4], they are useful for studying the early binding and entry stages of the virus. HPV PsV have been used as gene delivery vectors in the vaginal mucosa, respiratory tract, muscle and skin [5–9].

One notable feature of PsV-mediated gene delivery (hereafter referred to as infection) is the need for chemical or physical disruption or permeabilization of an epithelium to allow the virion access to the basement membrane. Specific binding of basement membrane heparan sulfate proteoglycans (HSPG) initiates a series of conformational changes in the virus leading to epithelial cell binding and, ultimately, delivery of encapsidated plasmid DNA into the cells [6, 10]. HSPG are widely recognized as the primary attachment factor necessary to promote HPV binding and infection both *in vitro* and *in vivo* [11–13]. Removal of HSPG from the cell surface or extracellular matrix (ECM) by heparinases prevents virus infection [12, 14], and cells deficient in HSPG are incapable of being infected [15, 16]. However, VLPs/PsV do not bind or infect the surfaces of intact cervicovaginal epithelium *in vivo* or primary keratinocytes *in vitro*, presumably because their cell surface HSPG lack the specific modifications required for capsid binding.

HSPG are ubiquitously expressed, and their importance in basement membrane remodeling is exemplified by the role they play in wound healing by facilitating repair and cellular repopulation. Though the need for physical access to the basement membrane may partially explain HPV's requirement for tissue disruption prior to infection, atraumatic infection of a mouse ovarian cancer model *in vitro* and *in vivo* suggests that other factors may affect HPV PsV targeting, such as cellular proliferation, inflammatory response, or recruitment and interaction with the immune system [17]. One bridging concept may be the comparison of tumor physiology to an "overhealing wound" where cellular and molecular changes involved in wound healing are exaggerated and extended in a pathological fashion [18]. In particular, overexpression, mutations and changes in HSPG sulfation patterns on tumors have been well-documented, potentially making them a target for HPV binding and infection [19–22]. While the tumor microenvironment lacks a structured basement membrane, it creates its own extracellular matrix. The ECM/tumor cell surface interface is enriched with HSPG and can play a role in cell signaling via binding growth factors and chemokines that influence cell growth, motility, adhesion and differentiation [23–25]. Changes in HSPG on tumors can lead to unregulated autocrine signaling loops that can promote tumorigenesis and angiogenesis.

Because of the unique aspects of the interactions of HPVs with their HSPG primary attachment factor and the documented changes in HSPG during tumor development, we have investigated the tropism of HPV binding and infection in multiple intact mouse tissues *in vivo*, in the NCI-60 cancer cell line panel *in vitro*, and in various tumor models *in vivo*. We found that HPV capsids fail to bind and infect normal, undisrupted tissues but do bind and infect a remarkably broad range of cancer cell lines *in vitro* and tumors *in vivo* in an HSPG-dependent manner.

MATERIALS AND METHODS

Cells and animals

Unless otherwise noted, all cells were cultured in DMEM supplemented with 10% FBS and were incubated at 37°C and 5% CO_2. NCI-60 cells lines were acquired from the Developmental Therapeutics Program at the National Cancer Institute (Frederick, MD) and were cultured in RPMI-1640, supplemented with 5% FBS and 2mM L-glutamine. Four lines from the NCI-60 panel were excluded due to inaccessibility or discrepancies with regard to cell origin (RS, MDA-N, MDA-MB-435, NCI/ADR-RES). Other cell sources: HeLa, CaSki, SiHa, C-33 A (ATCC, Manassas, VA), ES-2 (MPI Research, Mattawan, MI), A2780 cells (Sigma, St. Louis, MO), SHIN-3 DSR cells [26] were obtained from Dr. Hisataka Kobayashi (NCI, Bethesda, MD), bladder/uroepithelial cancer lines (J82, RT112, T24 and UMUC-5) were obtained from Dr. Piyush Agarwal (NCI, Bethesda, MD), head and neck tumor lines (CAL-33, HSC-3, UPCI-SCC-90, UPCI-SCC-154) were obtained from Dr. José Baselga (MSKCC, New York, NY) and NCI-H460-GFP cells were generated by TGen Drug Discovery (TD2, Scottsdale, AZ). Human tumor FM-108 (a poorly differentiated adenocarcinoma obtained from a metastasis to the diaphragm of a patient with a prior history of micropapillary serous carcinoma of the ovary) was a kind gift from Dr. Richard Roden (Johns Hopkins University, Baltimore, MD), and the tumor was obtained with patient consent under IRB protocol number J9883. MRI-H-207 (undifferentiated ovarian carcinoma) and MRI-H-258 (ovarian adenocarcinoma) were acquired from the NCI DCTD Tumor/Cell Line Repository (Frederick, MD) and were also obtained under IRB consent.

Female 6–8-week-old BALB/c and Athymic nude-$NCr^{nu/nu}$ mice (NCI, Frederick, MD) were housed in the NCI animal care facilities under pathogen-free conditions and maintained on standard rodent feed, with water supplied *ad libitum*, according to the current IACUC-approved documents. For the lung tumor orthotopic models, Athymic nude-$Foxn1^{nu}$ female mice aged 8–9 weeks were used (Harlan Laboratories, Indianapolis, IN) and housed at the TD2 facilities under the same conditions described above.

Pseudovirus (PsV) and virus-like particle (VLP) preparation and labeling

HPV16 VLP and PsV were generated, purified and titered as previously described [27]. Total L1 protein content was quantified using SDS-PAGE. Fluorescent labeling of VLP and PsV was performed using an Alexa Fluor 488 Protein Labeling Kit (AF488; Life Technologies, Carlsbad, CA) as described in Roberts, et al. [6]. Labeled particles were purified away from free dye either by filtration using a 2% 50–150mm agarose bead column (Agarose Bead Technologies, Tampa, FL) or OptiPrep density gradient (Sigma).

In vitro infectivity assay

NCI-60 screen—Cells were plated in duplicate into 96-well flat-bottomed, tissue-culture-treated plates at plating densities ranging from 5,000 to 40,000 cells/well based on the doubling time of individual cell lines. Cells were incubated for 24 hr prior to addition of PsV. Serial dilutions (1:10, 1:100 and 1:1000) of HPV16-GFP PsV (green fluorescent protein; titer: 1×10^9 IU/ml) were made in DPBS+0.8M NaCl, and 5 μl of each dilution, undiluted PsV and DPBS+0.8M NaCl alone were added to the cells. After 48 hr, cells were analyzed for GFP expression by flow cytometry using a FACSCanto II (BD, San Jose, CA). Data were analyzed using FlowJo v7 (TreeStar, Ashland, OR). The dilution of pseudovirus producing a percentage of GFP-positive cells within the linear range of the analysis (1–10%) was used to calculate the titer of HPV16-GFP PsV on each cell line. This value was then used to calculate relative infection compared to HeLa cells.

Heparin inhibition of infection—Cells (2×10^3) were plated in triplicate in a 96-well flat-bottom plate and incubated overnight. A dilution of HPV16-GFP PsV which infected cells in the range of 10–40% (amount varied between cell lines) was incubated with serially diluted concentrations of heparin (1mg/ml, three-fold serial dilutions to 0.001mg/ml; Sigma H4784) for 1 hr on ice. Samples were then added to the cells, and after 48 hr, cells were harvested and infection was assayed using flow cytometry as described above.

In vitro binding assay

Cells were dissociated and rotated on a nutating rocker at 37°C for 2–4 hr in 10ml of culture medium in order to recover their cell surface HSPG. AF488 VLP (2μg/ml) were pre-incubated with or without heparin (final concentration of 0.1mg/ml, Sigma H4784) for 1 hr on ice in 100μl PBS supplemented with 2% FBS (FACS buffer). For the modified heparin studies, a fixed amount of VLPs (2μg/ml) was pre-incubated as described above with serially diluted heparins: high molecular weight (HMW) heparin (H4784; Sigma) or N-desulfated, 2-O desulfated, 6-O desulfated or N-desulfated re-N-acetylated (all supplied from Galen Laboratory Supplies, Middletown, CT). Cells were counted, washed and resuspended in FACS buffer and plated in a 96-well round bottom plate at 1×10^5 cells/well, centrifuged and the supernatant removed. The virus and virus/heparin samples were added to the cells and incubated at 4°C for 1 hr. For heparinase studies, cells were allowed to recover for 2 hr at 37°C on a nutating rocker, and were then transferred to a round-bottom 96-well plate and incubated with serially diluted heparinases (I, II or III; Sigma) for an additional 2 hr at 37°C prior to addition of the VLPs directly to the cell/heparinase mixture and incubated as described above. After 1 hr of binding, cells were washed twice with FACS buffer, fixed with 4% paraformaldehyde, washed and resuspended in FACS buffer for analysis by flow cytometry as described above. Data are reported as either percent positive of total cells, or the geometric mean fluorescence was used to calculate the percent inhibition values.

In vivo VLP binding and PsV infection

Tissue tropism—Non-tumored BALB/c mice were treated with 2% nonoxynol-9 (N9; Ortho, Titusville, NJ) in 100μl PBS intraperitoneally (IP) 2 hr prior to virus inoculation.

AF488 VLP (62.5μg) was diluted in 100μl PBS and injected IP. Twenty-four hours post-injection, mice were euthanized and their organs harvested. Organs were snap-frozen in tissue freezing medium (EMS, Hatfield, PA), and 6μm sections were cut, mounted on SuperFrost Plus glass slides (Fisher, Waltham, MA) using ProLong Gold mounting medium with DAPI (Life Technology), and examined using a Zeiss LSM 510 confocal microscope (Zeiss, Oberkochen, Germany).

Tumor tropism ovarian model (fluorescent)—SHIN-3 DSR cells (1×10^7) were injected IP into nude mice. AF488 VLP (100μg) were administered 14 days later by IP injection. Tissues from animals treated with AF488 VLPs were harvested after 2 hr. To test inhibition of binding, AF488 VLP were pre-incubated with 100μl of 1% ι-carrageenan (Sigma) for 1 hr prior to injection. At the designated time points, the animals were euthanized, and the small intestine was removed from each animal and placed in a wheel formation on a black background for imaging. A Maestro device outfitted with a multispectral camera (PerkinElmer, Waltham, MA) with blue and green excitation filters paired with a 515-nm and a 580-nm long-pass emission filter, respectively, was used to obtain images from 500 nm to 900 nm in 10-nm wavelength increments. A spectral unmixing algorithm was applied to the composite images to determine the intensity and location of infection. Images were acquired, processed and analyzed using Nuance software (Perkin Elmer) and Image J (NIH, Bethesda, MD). After imaging, tissues were embedded in tissue freezing media (EMS), frozen, and 6μm sections were made and fixed to the slides for 10 min in −20°C ethanol (100%), then mounted and imaged as described above.

Tumor tropism ovarian model (luminescent)—SHIN-3 DSR cells were injected IP as described above. HPV16-Luc PsV (1×10^8 IU) was administered IP 14 days later +/− 1% ι-carrageenan as described above. After 48 hr, the animals were imaged using an IVIS100 imager (PerkinElmer). Luciferin-D substrate (200μl of a 15mg/ml stock; PerkinElmer) was injected IP, and after 3 min, bioluminescent images were acquired using a 30 sec exposure at medium binning. Data were analyzed using Living Image software (PerkinElmer), and values reported are average radiance within a region of interest drawn around the ventral area of each mouse.

Tumor tropism human xenograft ovarian models—Sterile tumor pieces ($1mm^3$; FM-108, MRI-H-207 and MRI-H-258) were implanted subcutaneously in 6–8 week old nude mice using a 13G cancer implant needle (Popper and Sons, Inc., New Hyde Park, NY). PsV was administered when tumors reached 7–15mm in diameter. PBS (50μl) or 2×10^7 IU HPV16-Luc or RFP PsV (in 50μl) was injected intratumorally. For luminescent imaging, animals were imaged after 48hr as described above. Tumors treated with RFP PsV were harvested three days post-infection and snap-frozen in tissue freezing medium (EMS). Six μm sections were cut and fixed onto glass slides in 2% paraformaldehyde, then mounted and imaged as described above.

Tumor tropism lung model—Animals received an intrathoracic administration of 1.5×10^6 H460-GFP cells. After 14 days, tumored and non-tumored mice were randomized and divided into groups receiving saline, empty HPV VLPs (100μg) or HPV16 PsV (Luc

and RFP; 25μg or 100μg) by intravenous (IV) administration. Whole body bioluminescent images were acquired as described above. Animals were then euthanized and their tissues (brain, lungs, draining lymph nodes, liver, and kidneys; ovaries in select animals if a signal was observed) were harvested for additional bioluminescent imaging (60 sec acquisition time). Tissues were fixed for 10min in 2% paraformaldehyde and frozen in tissue freezing medium (EMS) for microscopic analysis. Tissues were cut and sections mounted as described above. RFP and GFP expression was assessed using a Nikon Deconvolution Wide-Field Epifluorescence System (Nikon, Melville, NY).

RESULTS

Disruption is required for HPV binding to normal epithelial and mesothelial tissues

To extend our previous observation that HPV VLP do not bind to normal undisrupted tissues of the female genital tract [6], we chose to examine other tissues by inoculating mice with AF488 VLPs by intraperitoneal injection (IP). At 24 hr post-inoculation, no labeled virus could be detected on mouse peritoneal surfaces, including on the surface of the mouse peritoneum, intestine, uterus, liver, or ovary (Fig. 1a, c, e, g, and i). However, when mice were pre-treated IP with 2% nonoxynol-9 (N9) 2 hr prior to VLP treatment, virus was readily detected on organ surfaces (Fig. 1b, d, f, h, and j). These data extend previous findings that disruption of epithelial integrity is required for efficient HPV binding to a mesoderm-derived surface. Infection of intact tissues was also assessed using PsV transduction of an RFP-expressing plasmid (HPV16-RFP PsV) after local (IP, intranasal, intrabronchial) or intravenous application of the PsV (+/− N9 pre-treatment for locally administered conditions) followed by histological detection of red fluorescent cells. Tissues examined include: oropharyngeal mucosa, tongue, esophagus, small intestine, large intestine, anal canal, cornea and conjunctiva, trachea, bronchi, peritoneal surfaces, liver, spleen, bladder, uterus and ovaries. Although infection was readily detected after N9 pre-treatment, no infection was detected in intact mouse tissues, the one exception being an occasional infectious event observed in some sections of the lower lungs after intrabronchial instillation (Fig. S1). We conclude that binding to and infection of normal, undisrupted mouse tissue surfaces is minimal at best.

HPV16 PsV infect various cultured human tumor cell lines

To date, no systematic study of HPV PsV infectivity of a well-characterized panel of human tumor cell lines has been published. To investigate HPV16 PsV's ability to infect tumors of multiple origins, we assayed the infectivity of 56 tumor cell lines from the NCI-60 cancer cell panel. All of the tested cell lines were susceptible to HPV16 PsV infection, although their degree of susceptibility differed by more than four orders of magnitude (Fig. 2; Table S1). Generally, the epithelial-derived tumor types were more susceptible to infection compared to the non-epithelial types (CNS, lymphoid, melanoma).

HPV16 binding to, and infection of, tumor cell lines is competitively inhibited by heparin

To address the hypothesis that HPV tumor targeting activity was related to HSPG on the surface of the tumors, heparin (a highly sulfated form of heparan sulfate) was employed as a blocking agent for HPV binding on a panel of 24 tumor cell lines of diverse tissue origin

(cervical, head and neck, melanoma, lung, ovarian, uroepithelial). Heparin blocked binding of AF488 VLPs to all cell lines tested, indicating that HSPG likely play a role in the tumor tropism of HPV (Fig. 3a). To elucidate the particular sulfation patterns required for the interaction between HPV and the tumor cells, four modified heparins were examined to determine their comparative ability to prevent HPV binding. We chose to focus on epithelial derived ovarian and lung tumor lines along with a non-epithelial melanoma tumor line in order to examine HPV binding behavior on different cell lineages and to complement the *in vivo* studies. High molecular weight heparin (HMW; 16,000 Da), N-desulfated heparin, N-desulfated re-N-acetylated heparin, 2-O desulfated heparin and 6-O desulfated were tested. N-sulfation proved to be critical for HPV binding to all cell lines tested (Fig. 3b). Some reduced inhibition was noted with the N-desulfated re-N-acetylated heparin, indicating the importance of occupancy at the N-position. A minor reduction in binding was observed with the 2-O and 6-O desulfated heparins, however not to the degree noted with the N-desulfated heparin. Further, heparinases I, II and III were employed on these same cell lines to remove cell surface HSPG, and this treatment abrogated VLP binding in a dose-dependent manner (Fig. 3b).

Ovarian, lung and melanoma tumor line panels were tested for heparin's ability to block infection by HPV16-GFP PsV. A dose-dependent inhibition of infection was observed with each cell line, further implicating a role for HSPG in tumor infection by HPV PsV (Fig. 3c–e). Collectively, the data show that many human tumor cell lines were infected by HPV16 PsV, and even those that were poorly transduced were still capable of being bound by the HPV VLP.

HPV16 PsV specifically bind and infect human ovarian tumors in an HSPG dependent manner using an orthotopic murine model

We next studied the tumor tropism *in vivo* in order to determine if the tropism we had observed was an artifact of cell culture. The orthotopic SHIN-3 murine model of ovarian cancer was examined for its ability to be targeted by HPV after IP administration. Additionally, in order to address the role of HSPG *in vivo*, ι-carrageenan was used in lieu of heparin to block the VLP-HSPG interaction. To detect *in vivo* binding with the Maestro imaging system, a large amount of VLPs must be administered. The amount of heparin required to block this quantity of VLPs is toxic to the animals, therefore ι-carrageenan was employed for this purpose. Carrageenan is a heavily sulfated polysaccharide that prevents association of the HPV virion with HSPG, making it an exceptionally potent inhibitor of HPV binding and infection [6, 28]. AF488 VLP binding to, and infection of, a panel of tumor cell lines *in vitro* was effectively blocked by ι-carrageenan (Figs. S2 and S3a). SHIN-3 DSR cells, which express red fluorescent protein, were implanted IP into nude mice. After 14 days, animals received an IP injection of AF488 VLP +/− 1% ι-carrageenan, and 2 hr post-injection, tissues were analyzed *ex vivo*. We observed specific co-localization of AF488 VLPs (green signal) with the red fluorescent tumor cells within the peritoneal cavity, and binding was greatly diminished in the presence of ι-carrageenan (Fig. 4a). Minor autofluorescence in the green channel is an artifact of imaging tissues using this modality; however this background signal is consistent across all experimental conditions, and AF488 VLP localization is discernible over background. Upon microscopic assessment, the virus

was observed on the surface of the tumors, and this binding was effectively blocked by ι-carrageenan treatment (Fig. S3b).

IP injection of HPV16-GFP PsV into mice bearing SHIN-3 DSR tumors resulted in strong co-localization of green and red fluorescent signals, indicating specific PsV infection of the tumor cells (Fig. S4). To assess the HSPG dependency of PsV infection of tumors *in vivo*, SHIN-3 DSR-inoculated animals received an IP injection of HPV16-Luc PsV +/− 1% ι−carrageenan. After 48 hr, luminescence was measured, and a significant decrease in infection was noted in mice receiving ι−carrageenan (Fig. 4b; p=0.02). Taken together, these data indicate a role for HSPG in HPV binding to, and infection of, tumors *in vivo*.

HPV PsV specifically infect established human ovarian xenograft tumors but not healthy tissue in vivo

To address the possibility that HPV only specifically targets tissue culture-adapted tumor cells that may have developed specific HSPG modification in culture, we tested the ability of HPV16 PsV to infect primary human ovarian tumors. Tumors were implanted subcutaneously in immune-compromised mice, and RFP or Luc PsV was delivered intratumorally. Two days after PsV delivery, tumor-specific luciferase expression was observed (Fig. 5a). Non-tumored animals received a subcutaneous injection of PsV to serve as background controls. Additionally, upon microscopic evaluation of the tumors, RFP expression was observed in the extracted tumors (Fig. 5b) but was not observed in the adjacent normal tissue (data not shown). These results imply that human tumors that have evolved entirely *in vivo* are also selectively infected by HPV PsV.

HPV PsV specifically infect both primary and metastatic human lung tumors after intravenous delivery

Having demonstrated that local and direct HPV delivery to tumors was feasible, we then examined the tumor targeting ability of the PsV after systemic administration (IV). To test this possibility, we used an orthotopic lung tumor model in which human H460-GFP cells (stably expresses green fluorescent protein) are implanted into the thoracic cavity of nude mice. Two weeks post-implantation, IV injections of saline, empty HPV16 VLP or PsV (25μg or 100μg) consisting of HPV16-RFP and HPV16-Luc PsV were administered, and animals were imaged for infection. Whole body and lung imaging for bioluminescent signal indicated that HPV16 preferentially targeted the tumors in a dose-dependent manner (Fig. 6a and 6b, respectively). *Ex vivo* imaging of individual organs shows preferential infection in the lungs of tumored animals and the draining lymph nodes and ovaries of some tumored animals (Fig. S5). Microscopic analysis was performed on several tissues harvested from the non-tumored and tumored animals (lungs, mediastinal lymph nodes, brain, liver, spleen, kidneys and the ovaries of one mouse that appeared luciferase-positive). Tumor cells were detected by GFP expression (expression levels varied throughout the tumor), and HPV16 PsV infection was demarcated by RFP expression. Co-localization of HPV infection was dispersed throughout the primary lung tumors (Fig. 6c). With the exception of a few positive events found in luminal cells of the liver and spleens of three animals (data not shown), non-specific infection was not observed in the normal mouse tissues. Interestingly, metastatic nodules were observed in some animals in the draining lymph nodes and ovaries (as

demonstrated by GFP-expressing tumor cells); in these instances, RFP expression was also observed, indicating that systemically administered HPV PsV was capable of targeting metastases at distant sites (Fig. 6c, ovaries, lymph nodes).

DISCUSSION

The results of this study reveal interesting aspects of tumor biology and describe a reagent with the potential to identify and target, for detection and treatment, a broad spectrum of tumor types. Biologically, our results imply that there is a strong, previously unappreciated, selective pressure on tumors of many types to evolve a specific pattern of HSPG modifications mimicking a pattern normally found on the basement membrane but not the apical surfaces of normal tissues. While the precise tumor and basement membrane HSPG modification pattern recognized by the HPV capsids remains to be identified, the binding and infection inhibition experiments with the heparin derivatives implicate heparan sulfate N-sulfation as a critical component for binding to tumors and, as previously reported, to the basement membrane [12]. Importantly, our *in vitro* observations were confirmed using primary human tumors implanted in mice, indicating that the tumor tropism we observed was not an artifact of *in vitro* passaged cells. We have observed similar results using murine tumors in immune-competent mice, and studies examining spontaneously arising tumors are planned.

HSPGs play an important role in wound healing by facilitating repair and cellular repopulation. HSPGs expressed on the cell surface (syndecans and glypicans) and in the ECM (perlecans) play several roles in growth factor autocrine and paracrine signaling loops within the local microenvironment. HSPGs can serve several functions, namely 1) they sequester soluble growth factors within the ECM such that these factors are poised for release upon stimulation; 2) they mediate adhesion molecule ligand interactions and signaling involved in cell motility and migration; 3) they are able to bind and initiate oligomerization of growth factors promoting a bioactive state; and 4) they prevent the functionality of coagulation factors which can enable neovascularization [23, 29]. In the setting of cancer, each of these characteristics can simultaneously serve to promote tumorigenic growth and metastasis [24, 25, 30, 31].

We speculate that the normal restriction of epithelial proliferation to the basal layer may be due, at least in part, to a requirement for signals derived from the specifically modified forms of HSPG normally found only on the basement membrane. Proliferation of tumor cells in the absence of basement membrane attachment may therefore be dependent on evolution of similar HSPG modifications on their cell surfaces and/or the ECM they produce. Contrary to primary keratinocytes' inability to be bound or infected by HPV, it is interesting to note that many non-tumorigenic cell lines immortalized by *in vitro* passage are readily bound and infected by the HPV capsids [11–13], suggesting that the requisite HSPG modifications may develop at an early stage in culture in the absence of a basement membrane. However, it is unknown whether this is also true of intraepithelial neoplasia and other premalignant lesions *in vivo*.

Our finding that HPV preferentially targets tumor cells *in vivo* may temper causal inferences in some epidemiology studies that detect HPV DNA in human tumors. HPV infection is clearly established as the primary cause of cervical and several other anogenital cancers, based upon the criteria of clonality, consistent viral oncogene expression and the fact that prospective studies have shown that infection precedes development of premalignant neoplasia and progression to cancer [32]. However, the causal association of cutaneous HPV with non-melanoma skin cancer is less well established. Given the near ubiquitous detection of Beta and Gamma HPVs on human skin, it seems possible that their frequent detection in a minority of skin cancer cells might be due to secondary infection of established tumors [33]. We have not yet fully evaluated the tumor tropism of cutaneous HPV types, but the tropism of HPV5 and the animal cutaneous papillomavirus types from cows (BPV1), rabbits (CRPV) and mice (MusPV1) is similar to that of HPV16 (our unpublished observations). HPV virions have also been detected in circulating blood and are capable of binding to peripheral blood mononuclear cells of otherwise healthy individuals in several studies [34–37]. It is plausible to imagine a scenario in which free or cell-associated HPV virions in the circulation could home to a pre-existing tumor, leading to non-productive infection. This scenario might explain reports of sporadic detection of HPV DNA in various tumor types, including lung [38, 39], breast [40], prostate [41], colon [42, 43] and bladder [44].

The ability of HPV capsids to home to both primary and metastatic tumors, even after intravenous instillation, suggests a variety of applications, both in diagnostics and therapeutics, as broad-spectrum “pan-tumor” targeting reagents. We have demonstrated that coupling small molecules such as dyes to the HPV VLP does not adversely affect its targeting ability, nor alter its reliance upon HSPGs. Imaging dyes (ICG, FITC) or radio isotopes (gamma emitters) could be easily attached to the VLP and used for live, *in situ* imaging of tumors and metastases upon systemic administration. Further, adding a cytotoxic reagent or pro-drug could target the tumor for killing while leaving healthy cells intact and reducing the systemic toxicity often associated with chemotherapy and radiotherapy. An alternative approach, recently initiated by Hung et al (2012) [17], would be to encapsidate within the HPV PsV plasmid DNA encoding cytotoxic genes such as thymidine kinase or other “suicide genes” that either kill the infected tumor cells or increase their sensitivity to chemotherapeutics.

Potential shortcomings of using HPV to target tumors may include: 1) the presence of neutralizing antibodies due to natural infection or vaccination with an HPV VLP vaccine and 2) HPV virions may bind immune cells [34, 35] and therefore fewer virions may reach the tumor and/or trigger a systemic innate immunological response. To avoid neutralization in vaccinated individuals, we are further evaluating other human and animal papillomavirus types for their tumor tropism. Thus far, all types demonstrate tropism similar to HPV16 *in vitro* (our unpublished data). With regard to immune cell binding particularly after systemic administration, there is no reason to believe that it will impact the tumor homing as was demonstrated in mice. No toxicity has been observed in mice that have received up to 200μg IV. Additionally, blood chemistry and blood counts measured in mice prior to IV injection and 24hr post-injection show no major differences, indicating that, at least in the murine

model, systemic administration was well tolerated and did not impact overall immune status. Toxicity studies in other animal models are currently ongoing to further address these issues.

Precedent exists for using antibodies, viruses and bacteria in the approaches described above with regard to tumor therapy. However, these strategies rely on very specific receptor expression (i.e. HER2), require modifications to the agent in question, have substantial interactions with normal tissue and/or are tumor type restricted. Importantly, the HPV VLP (or PsV) requires no modification, as the tumor tropism is an innate feature of the virus and serves as a means to exploit the HPSG modifications found on many tumor types but not normal intact tissues. We are continuing to investigate the particular heparan sulfate modifications and patterns that mediate HPV VLP binding to the tumors. Exploration of the delivery of drugs and nuclear isotopes are also underway in various tumor models.

Supplementary Material

Refer to Web version on PubMed Central for supplementary material.

ACKNOWLEDGMENTS

We gratefully acknowledge Drs. Hisataka Kobayashi and Richard Roden for their kind gifts of the SHIN-3 DSR cells and the FM-108 xenograft, respectively. JNR, DRL and JTS are inventors on US government owned patent pertaining to this technology and licensed to Aura Biosciences. RCK is an employee and EdLP is founder, CEO and employee of Aura Bioscience. This work was funded by the NIH intramural program and Aura Biosciences.

Abbreviations used

HPV	human papillomavirus
HSPG	heparan sulfate proteoglycans
VLP	virus-like particle
PsV	pseudovirus
Luc	firefly luciferase
GFP	green fluorescent protein
RFP	red fluorescent protein
DSR	ds-Red fluorescent protein
ECM	extracellular matrix
AF488	Alexa Fluor 488
N9	nonoxynol-9
IU	infectious units
IP	intraperitoneal
IV	intravenous

REFERENCES

1. Ferlay J, Soerjomataram II, Dikshit R, Eser S, Mathers C, Rebelo M, Parkin DM, Forman DD, Bray F. Cancer incidence and mortality worldwide: sources, methods and major patterns in GLOBOCAN 2012. International Journal of Cancer. 2014
2. Jayson GC, Kohn EC, Kitchener HC, Ledermann JA. Ovarian cancer. Lancet. 2014
3. Reck M, Heigener DF, Mok T, Soria JC, Rabe KF. Management of non-small-cell lung cancer: recent developments. Lancet. 2013; 382:709–719. [PubMed: 23972814]
4. Buck CB, Pastrana DV, Lowy DR, Schiller JT. Efficient intracellular assembly of papillomaviral vectors. Journal of Virology. 2004; 78:751–757. [PubMed: 14694107]
5. Gambhira R, Karanam B, Jagu S, Roberts JN, Buck CB, Bossis I, Alphs H, Culp T, Christensen ND, Roden RB. A protective and broadly cross-neutralizing epitope of human papillomavirus L2. Journal of Virology. 2007; 81:13927–13931. [PubMed: 17928339]
6. Roberts JN, Buck CB, Thompson CD, Kines R, Bernardo M, Choyke PL, Lowy DR, Schiller JT. Genital transmission of HPV in a mouse model is potentiated by nonoxynol-9 and inhibited by carrageenan. Nature Medicine. 2007; 13:857–861.
7. Graham BS, Kines RC, Corbett KS, Nicewonger J, Johnson TR, Chen M, LaVigne D, Roberts JN, Cuburu N, Schiller JT, Buck CB. Mucosal delivery of human papillomavirus pseudovirus-encapsidated plasmids improves the potency of DNA vaccination. Mucosal Immunology. 2010; 3:475–486. [PubMed: 20555315]
8. Cuburu N, Graham BS, Buck CB, Kines RC, Pang YY, Day PM, Lowy DR, Schiller JT. Intravaginal immunization with HPV vectors induces tissue-resident CD8+ T cell responses. The Journal of Clinical Investigation. 2012; 122:4606–4620. [PubMed: 23143305]
9. Handisurya A, Day PM, Thompson CD, Buck CB, Kwak K, Roden RB, Lowy DR, Schiller JT. Murine skin and vaginal mucosa are similarly susceptible to infection by pseudovirions of different papillomavirus classifications and species. Virology. 2012; 433:385–394. [PubMed: 22985477]
10. Kines RC, Thompson CD, Lowy DR, Schiller JT, Day PM. The initial steps leading to papillomavirus infection occur on the basement membrane prior to cell surface binding. Proceedings of the National Academy of Sciences of the United States of America. 2009; 106:20458–20463. [PubMed: 19920181]
11. Knappe M, Bodevin S, Selinka HC, Spillmann D, Streeck RE, Chen XS, Lindahl U, Sapp M. Surface-exposed amino acid residues of HPV16 L1 protein mediating interaction with cell surface heparan sulfate. The Journal of Biological Chemistry. 2007; 282:27913–27922. [PubMed: 17640876]
12. Johnson KM, Kines RC, Roberts JN, Lowy DR, Schiller JT, Day PM. Role of heparan sulfate in attachment to and infection of the murine female genital tract by human papillomavirus. Journal of Virology. 2009; 83:2067–2074. [PubMed: 19073722]
13. Surviladze Z, Dziduszko A, Ozbun MA. Essential roles for soluble virion-associated heparan sulfonated proteoglycans and growth factors in human papillomavirus infections. PLoS Pathogens. 2012; 8:e1002519. [PubMed: 22346752]
14. Giroglou T, Florin L, Schafer F, Streeck RE, Sapp M. Human papillomavirus infection requires cell surface heparan sulfate. Journal of virology. 2001; 75:1565–1570. [PubMed: 11152531]
15. Joyce JG, Tung JS, Przysiecki CT, Cook JC, Lehman ED, Sands JA, Jansen KU, Keller PM. The L1 major capsid protein of human papillomavirus type 11 recombinant virus-like particles interacts with heparin and cell-surface glycosaminoglycans on human keratinocytes. The Journal of Biological Chemistry. 1999; 274:5810–5822. [PubMed: 10026203]
16. Day PM, Lowy DR, Schiller JT. Heparan sulfate-independent cell binding and infection with furin-precleaved papillomavirus capsids. Journal of Virology. 2008; 82:12565–12568. [PubMed: 18829767]
17. Hung CF, Chiang AJ, Tsai HH, Pomper MG, Kang TH, Roden RR, Wu TC. Ovarian cancer gene therapy using HPV-16 pseudovirion carrying the HSV-tk gene. PloS One. 2012; 7:e40983. [PubMed: 22815887]
18. Schafer M, Werner S. Cancer as an overhealing wound: an old hypothesis revisited. Nature Reviews Molecular Cell Biology. 2008; 9:628–638. [PubMed: 18628784]

19. Liu D, Shriver Z, Venkataraman G, El Shabrawi Y, Sasisekharan R. Tumor cell surface heparan sulfate as cryptic promoters or inhibitors of tumor growth and metastasis. Proceedings of the National Academy of Sciences of the United States of America. 2002; 99:568–573. [PubMed: 11805315]
20. Esko JD, Lindahl U. Molecular diversity of heparan sulfate. The Journal of Clinical Investigation. 2001; 108:169–173. [PubMed: 11457867]
21. Sanderson RD, Yang Y, Kelly T, MacLeod V, Dai Y, Theus A. Enzymatic remodeling of heparan sulfate proteoglycans within the tumor microenvironment: growth regulation and the prospect of new cancer therapies. Journal of Cellular Biochemistry. 2005; 96:897–905. [PubMed: 16149080]
22. Hammond E, Khurana A, Shridhar V, Dredge K. The Role of Heparanase and Sulfatases in the Modification of Heparan Sulfate Proteoglycans within the Tumor Microenvironment and Opportunities for Novel Cancer Therapeutics. Frontiers in Oncology. 2014; 4:195. [PubMed: 25105093]
23. Tumova S, Woods A, Couchman JR. Heparan sulfate proteoglycans on the cell surface: versatile coordinators of cellular functions. The International Journal of Biochemistry & Cell Biology. 2000; 32:269–288. [PubMed: 10716625]
24. Liu D, Shriver Z, Qi Y, Venkataraman G, Sasisekharan R. Dynamic regulation of tumor growth and metastasis by heparan sulfate glycosaminoglycans. Seminars in Thrombosis and Hemostasis. 2002; 28:67–78. [PubMed: 11885027]
25. Fuster MM, Wang L. Endothelial heparan sulfate in angiogenesis. Progress in Molecular Biology and Translational Science. 2010; 93:179–212. [PubMed: 20807646]
26. Hama Y, Urano Y, Koyama Y, Kamiya M, Bernardo M, Paik RS, Shin IS, Paik CH, Choyke PL, Kobayashi H. A Target Cell-Specific Activatable Fluorescence Probe for In vivo Molecular Imaging of Cancer Based on a Self-Quenched Avidin-Rhodamine Conjugate. Cancer Research. 2007; 67:2791–2799. [PubMed: 17363601]
27. Buck, CB.; Thompson, CD. Bonifacino, Juan S., et al. Current Protocols in Cell Biology / editorial board. 2007. Production of papillomavirus-based gene transfer vectors. Chapter 26: Unit 26 1.
28. Buck CB, Thompson CD, Roberts JN, Muller M, Lowy DR, Schiller JT. Carrageenan is a potent inhibitor of papillomavirus infection. PLoS Pathogens. 2006; 2:e69. [PubMed: 16839203]
29. Lindahl U, Kjellen L. Pathophysiology of heparan sulphate: many diseases, few drugs. Journal of Internal Medicine. 2013; 273:555–571. [PubMed: 23432337]
30. Sasisekharan R, Shriver Z, Venkataraman G, Narayanasami U. Roles of heparan-sulphate glycosaminoglycans in cancer. Nature Reviews Cancer. 2002; 2:521–528. [PubMed: 12094238]
31. Fuster MM, Esko JD. The sweet and sour of cancer: glycans as novel therapeutic targets. Nature Reviews Cancer. 2005; 5:526–542. [PubMed: 16069816]
32. Bosch FX, Lorincz A, Munoz N, Meijer CJ, Shah KV. The causal relation between human papillomavirus and cervical cancer. Journal of Clinical Pathology. 2002; 55:244–265. [PubMed: 11919208]
33. Accardi R, Gheit T. Cutaneous HPV and skin cancer. Presse Medicale (Paris, France : 1983). 2014; 43:e435–e435.
34. Da Silva DM, Velders MP, Nieland JD, Schiller JT, Nickoloff BJ, Kast WM. Physical interaction of human papillomavirus virus-like particles with immune cells. International Immunology. 2001; 13:633–641. [PubMed: 11312251]
35. Lenz P, Thompson CD, Day PM, Bacot SM, Lowy DR, Schiller JT. Interaction of papillomavirus virus-like particles with human myeloid antigen-presenting cells. Clinical Immunology. 2003; 106:231–237. [PubMed: 12706410]
36. Bodaghi S, Wood LV, Roby G, Ryder C, Steinberg SM, Zheng ZM. Could human papillomaviruses be spread through blood? Journal of Clinical Microbiology. 2005; 43:5428–5434. [PubMed: 16272465]
37. Chen AC, Keleher A, Kedda MA, Spurdle AB, McMillan NA, Antonsson A. Human papillomavirus DNA detected in peripheral blood samples from healthy Australian male blood donors. Journal of Medical Virology. 2009; 81:1792–1796. [PubMed: 19697401]

38. Ciotti M, Giuliani L, Ambrogi V, Ronci C, Benedetto A, Mineo TC, Syrjanen K, Favalli C. Detection and expression of human papillomavirus oncogenes in non-small cell lung cancer. Oncology Reports. 2006; 16:183–189. [PubMed: 16786144]

39. Cheng YW, Wu MF, Wang J, Yeh KT, Goan YG, Chiou HL, Chen CY, Lee H. Human papillomavirus 16/18 E6 oncoprotein is expressed in lung cancer and related with p53 inactivation. Cancer Research. 2007; 67:10686–10693. [PubMed: 18006810]

40. Kan CY, Iacopetta BJ, Lawson JS, Whitaker NJ. Identification of human papillomavirus DNA gene sequences in human breast cancer. British Journal of Cancer. 2005; 93:946–948. [PubMed: 16222323]

41. Martinez-Fierro ML, Leach RJ, Gomez-Guerra LS, Garza-Guajardo R, Johnson-Pais T, Beuten J, Morales-Rodriguez IB, Hernandez-Ordonez MA, Calderon-Cardenas G, Ortiz-Lopez R, Rivas-Estilla AM, Ancer-Rodriguez J, et al. Identification of viral infections in the prostate and evaluation of their association with cancer. BMC Cancer. 2010; 10:326. [PubMed: 20576103]

42. Bodaghi S, Yamanegi K, Xiao SY, Da Costa M, Palefsky JM, Zheng ZM. Colorectal papillomavirus infection in patients with colorectal cancer. Clinical Cancer Research. 2005; 11:2862–2867. [PubMed: 15837733]

43. Damin DC, Ziegelmann PK, Damin AP. Human papillomavirus infection and colorectal cancer risk: a meta-analysis. Colorectal Disease. 2013; 15:e420–e428. [PubMed: 23895733]

44. Kim SH, Joung JY, Chung J, Park WS, Lee KH, Seo HK. Detection of human papillomavirus infection and p16 immunohistochemistry expression in bladder cancer with squamous differentiation. PloS One. 2014; 9:e93525. [PubMed: 24675970]

Novelty and Impact

We demonstrate the broad tumor tropism of HPV both *in vitro* and *in vivo*, in part due to over-expression and possible modification of HSPGs on tumors. Healthy intact tissue is resistant to HPV binding, thus making HPV particles loaded with contrast agents or drugs useful tools for targeting tumors for diagnostic and therapeutic applications.

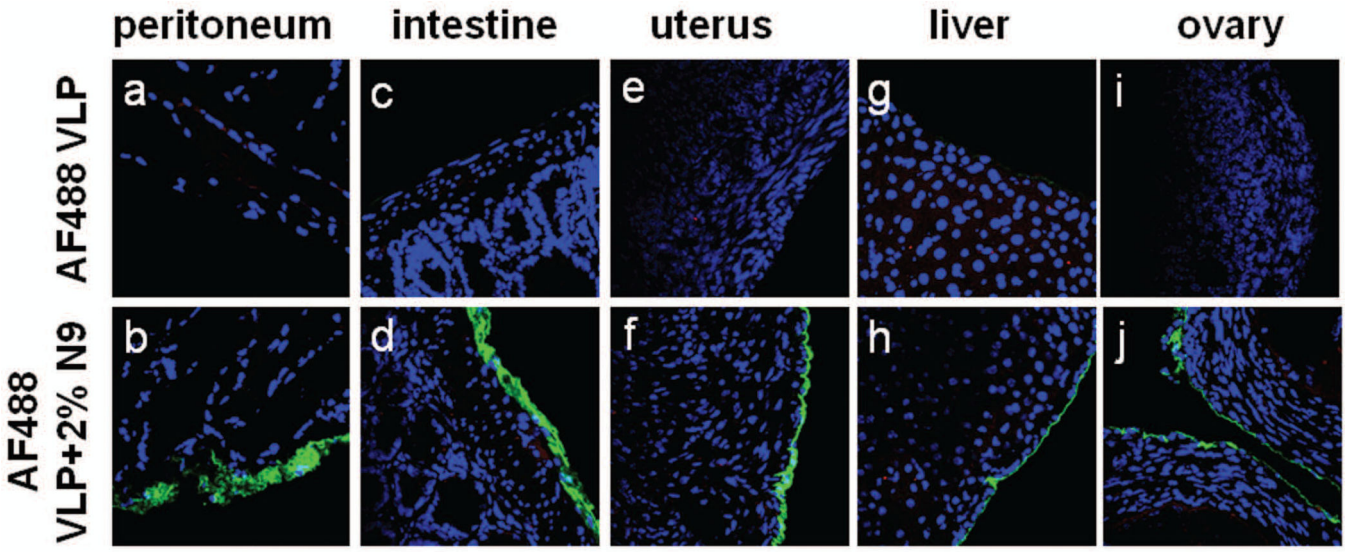

Figure 1.

Normal tissues are refractory to HPV binding *in vivo* unless traumatized. HPV VLPs coupled to Alexa Fluor 488 (AF488) were administered intraperitoneally into naïve animals or animals that had been pre-treated with 2% nonoxynol-9 (N9) via the same route. After 24hr, the tissues were harvested, frozen, sectioned and VLPs were imaged directly by detecting AF488 signal microscopically (Blue=DAPI, Green=VLP). The first row depicts tissues from animals that did not receive N9 (panels, a, c, e, g and i) and the second row depicts tissues from animals after N9 pre-treatment (b, d, f, h and j). Images are representative of 3 animals.

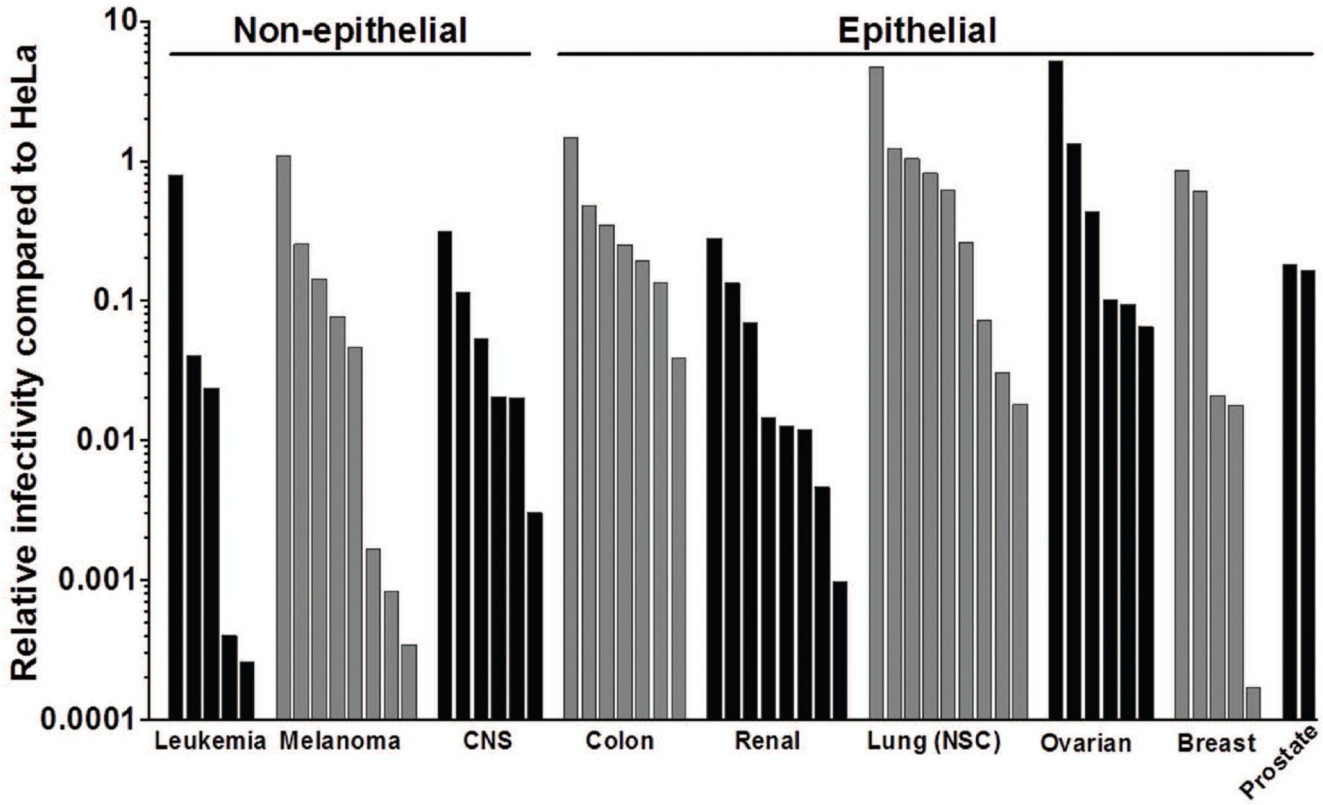

Figure 2.

HPV-16 infects many human tumor cell lines. A panel of 56 human tumor cell lines were infected with HPV16-GFP PsV, and GFP signal was measured 72hr later. HeLa cells served as controls and were used to calculate the relative infection of each cell type and these values are plotted (see Table S1 for raw data values). Cell lines are ordered as follows: Leukemia/Lymphoid (K-562, RPMI 8226, CCRF-CEM, MOLT-4, HL-60); Melanoma (SK-MEL-2, UACC-62, SK-MEL-5, MALME-3M, LOXIMVI, UACC-257, M14, SK-MEL-28); Central Nervous System (CNS; SNB-19, U251, SF-268, SF-539, SNB-75, SF-295); Colon (HCC-2998, HCT-15, KM12, COLO205, HCT-116, HT29, SW-620); Renal (TK-10, CAKI-1, A498, 786-0, SN12C, ACHN, UO-31, RXF-393); Lung (NCI-H522, NCI-H23, NCI-H322M, NCI-H460, EKVX, A549, HOP-62, HOP-92, NCI-H226); Ovarian (OVCAR-3, OVCAR-4, IGROV1, OVCAR-8, OVCAR-5, SK-OV-3); Breast (T47D; MCF7, HS578T, BT-549, MDA-MB-231); Prostate (PC-3, DU-145).

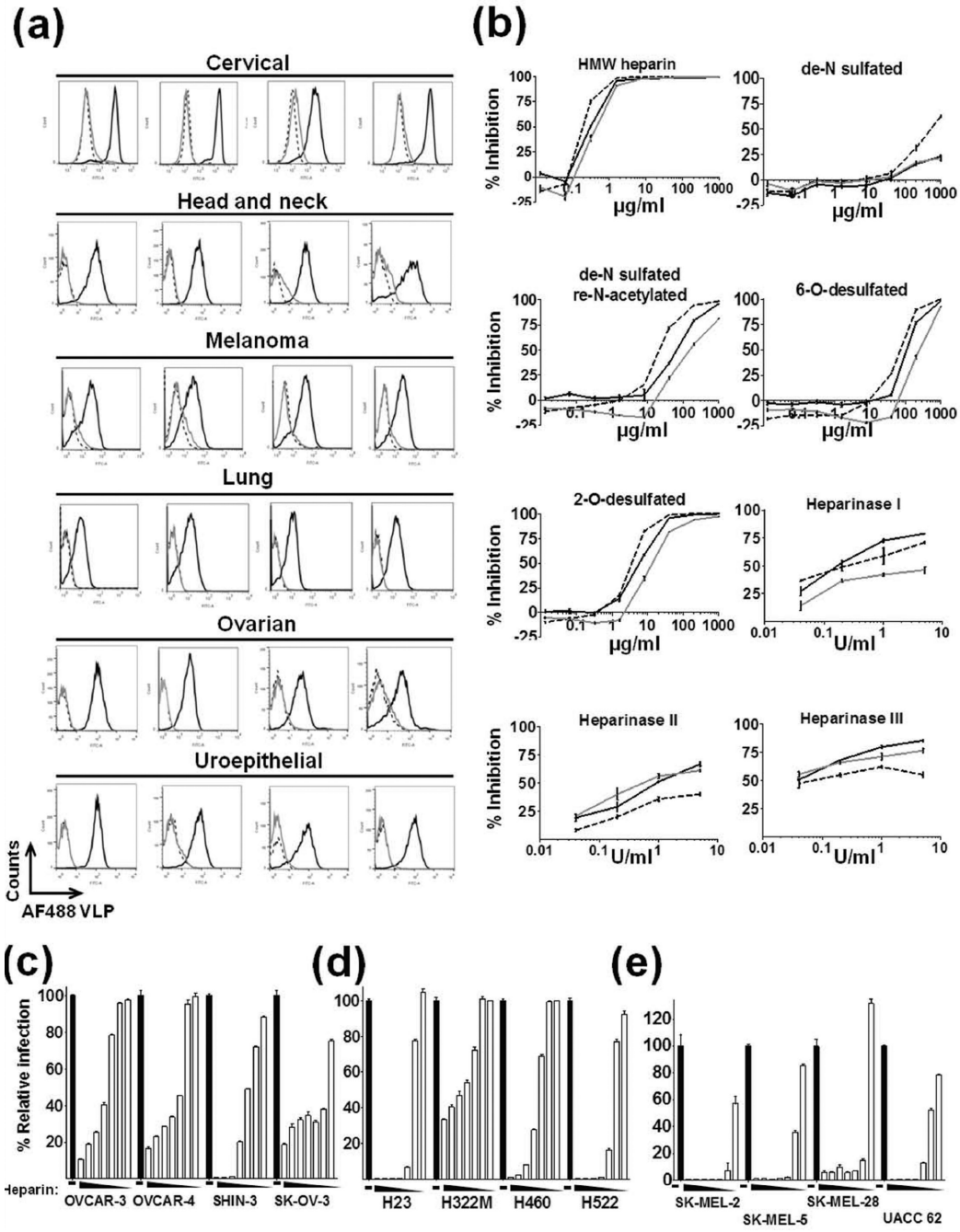

Figure 3.

HPV16 VLP binding to and PsV infection of tumor cell lines is competitively inhibited by heparin. (a) Flow histograms of 2µg/ml AF488 VLPs bound to cells in the absence (black line) or presence (gray line) of 1mg/ml heparin (negative control, dashed line). Tumor cell lines tested: Cervical (HeLa, SiHa, C 33A, CaSki); Head and Neck (CAL-33, HSC-3, UPCI SCC-90, UPCI SCC-154); Melanoma (SK-MEL 2, SK-MEL 5, SK-MEL 28, UACC-62); Lung (NCI-H23, NCI-H322M, NCI-H460, NCI-H522); Ovarian (SK-OV-3, A2780, OVCAR-3, OVCAR-4); Uroepithelial (J82, RT112, T24, UMUC-5). (b) Dose response

inhibition of binding using modified heparins and heparinases on SK-OV-3 (ovarian, solid black line), NCI-H460 (lung, solid gray line) and SK-MEL-2 (melanoma, dashed black line) (experiment performed in triplicate, data representative of two experiments). Dose response of heparin inhibition of PsV infection of (c) ovarian, (d) lung and (e) melanoma cancer cell line panels. Heparin concentration begins with 1mg/ml and is serially diluted three-fold (experiment performed in triplicate, data representative of two experiments).

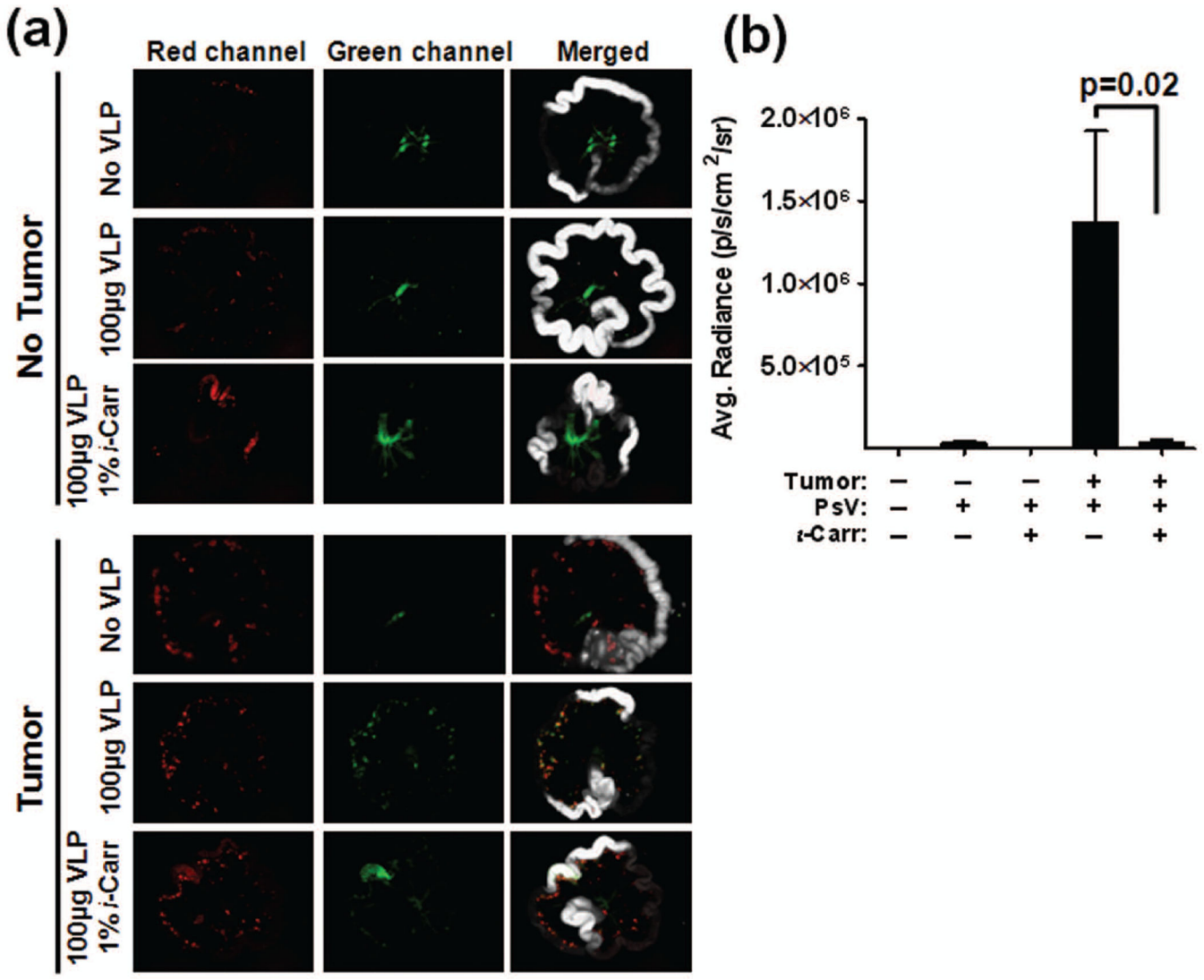

Figure 4.

ι-Carrageenan blocks binding of HPV to SHIN-3 DSR ovarian tumors *in vivo*. Non-tumored and SHIN-3 DSR tumored mice were examined for AF488 VLP binding (a) and HPV16-Luc PsV infection (b). (a) Animals received an intraperitoneal injection of PBS, 100µg AF488 VLP or 100µg AF488 VLP+1% ι-carrageenan. 2hr post-injection, the small intestines was removed and placed in a "wheel" formation for *ex vivo* fluorescent imaging. White, Red (tumor), and Green (VLP) channels were collected and individual as well as merged images are pictured. (b) Tumored and non-tumored animals received an intraperitoneal injection of 1×10^8 IU of HPV16-Luc PsV in 100µl PBS +/− 1% ι-carrageenan. 48hr later, luciferin substrate was administered and bioluminescence was measured. A region of interest was drawn around the peritoneal cavity and the average radiance was calculated. All data are representative of n ≥5/group.

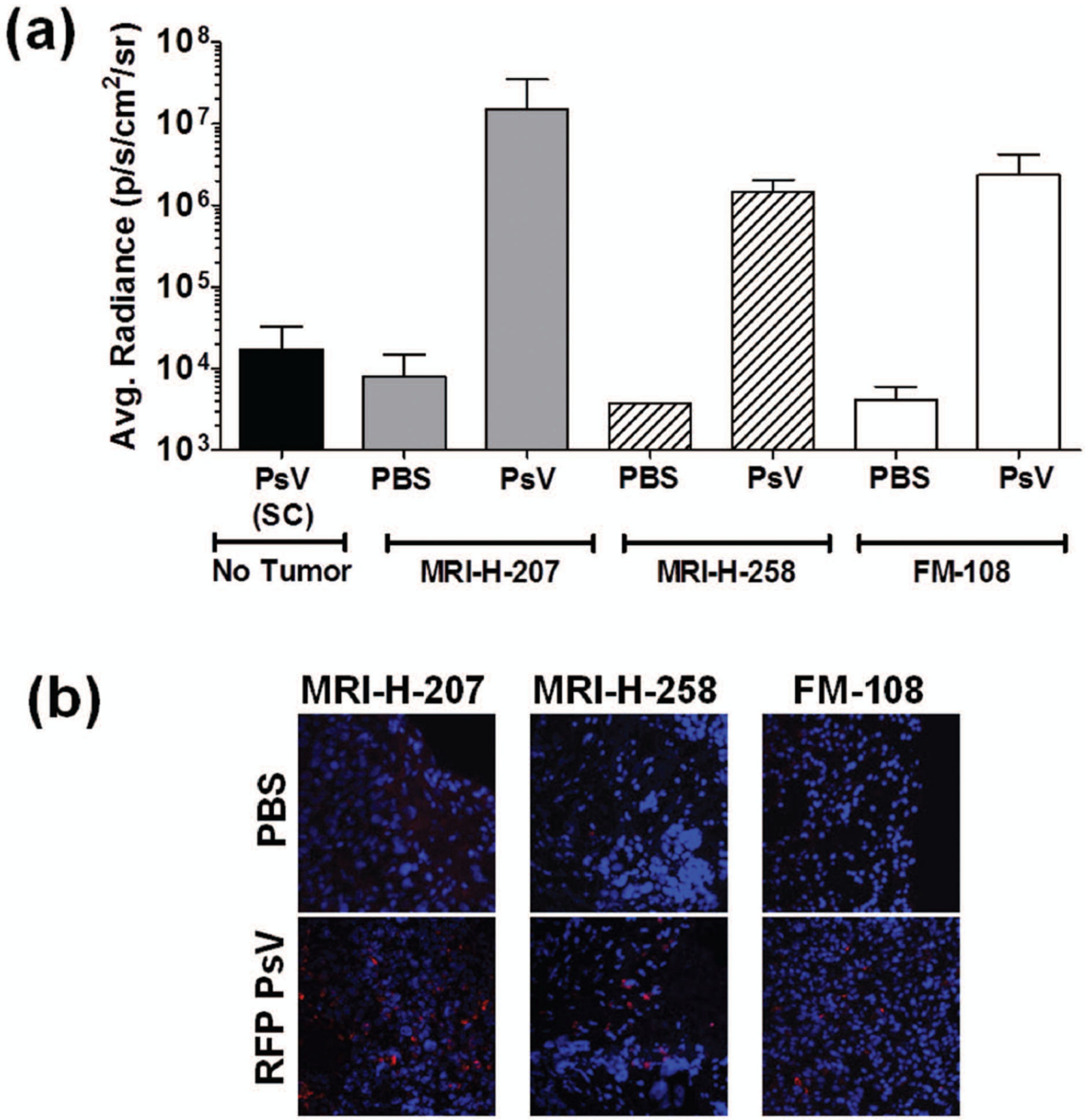

Figure 5.

HPV pseudoviruses infect established xenograft human ovarian tumors but not healthy tissue *in vivo*. Human ovarian tumors passaged only in immune-compromised animals were subcutaneously implanted. When tumors were between 7–15mm in diameter, animals received an intratumoral injection of 50μl PBS or 50μl 2×10^7 IU HPV16-Luc (a) or RFP (b) PsV. Non-tumored animals received a subcutaneous injection in their hind flank. Luminescence values are reported as average radiance (a) and micrographs (b) depict RFP expression (Red=RFP; Blue=DAPI) as a readout for PsV infection. n= 2–11/group.

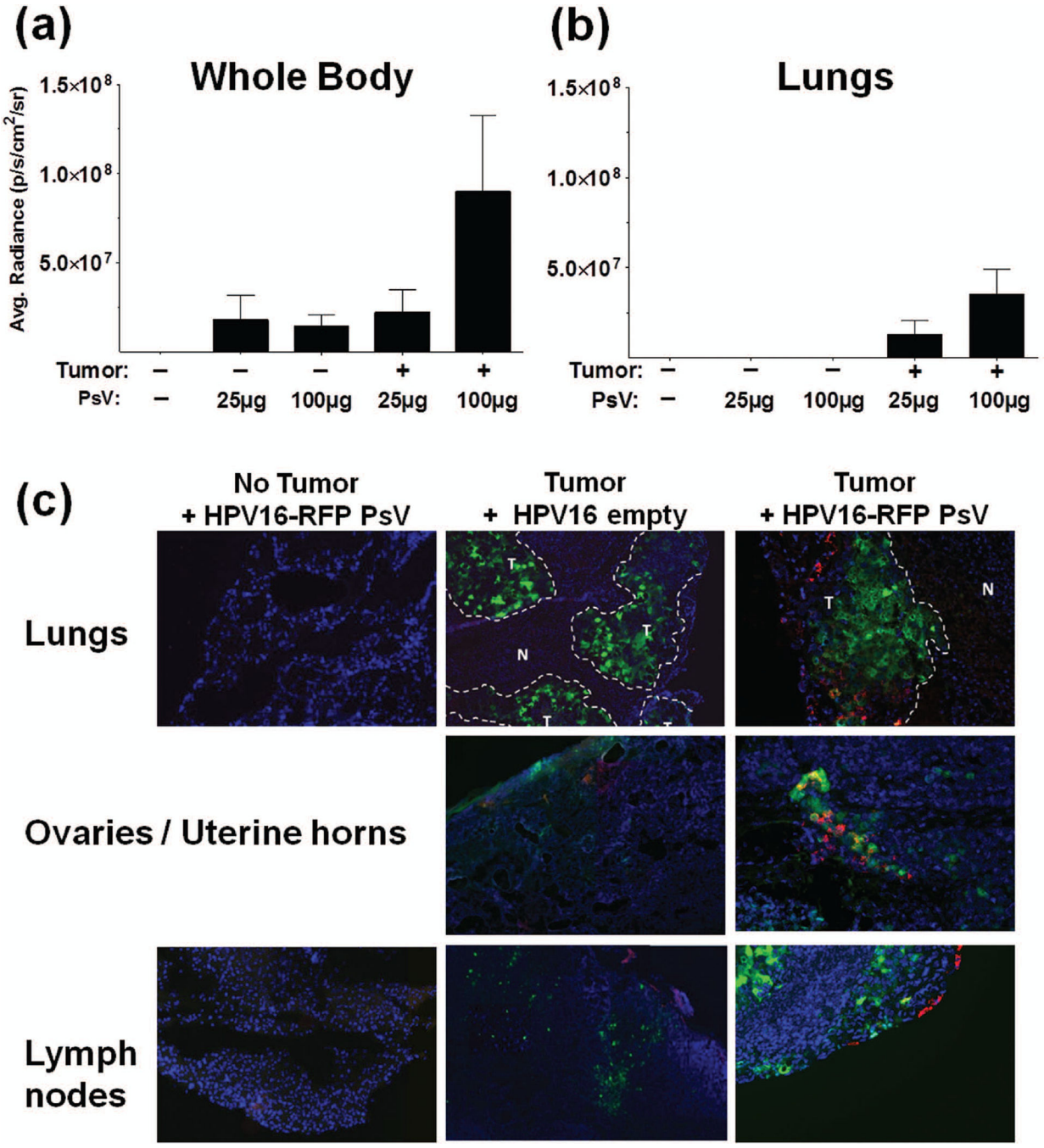

Figure 6.

HPV pseudoviruses infect orthotopic lung tumors after systemic administration (IV). Non-tumored or orthotopically H460-GFP tumored animals received intravenous injection of 25µg or 100µg each of HPV16-Luc 48hr before imaging (a) and (b) and HPV16-RFP 72hr before imaging (c). Whole body luminescent images were first acquired (a) followed by imaging of individual organs ((b) depicts lungs) (signal decreases rapidly upon euthanasia and dissection; Fig. S5 shows raw images of all organs). After imaging, tissues were frozen, sectioned and examined by fluorescent microscopy (c). Images are merged channels,

Blue=DAPI, Red=PsV infection and Green=tumor (faint in some images). T= tumor, N= normal. n=7–10/group.